Amino Acids (2007) 32: 593–602
DOI 10.1007/s00726-006-0424-9
Printed in The Netherlands

Amino Acids

Kinetic and proteomic analyses of *S*-nitrosoglutathione-treated hexokinase A: consequences for cancer energy metabolism

S. Miller, C. Ross-Inta, and **C. Giulivi**

Department of Molecular Biosciences, University of California, Davis, CA, U.S.A.

Received December 13, 2005
Accepted May 12, 2006
Published online October 20, 2006;

Summary. Mammalian hexokinase (HXK) is found at the outer mitochondrial membrane, exposed to mitochondrial oxygen- and nitrogen-radicals. Given the important role of this enzyme in metabolic pathways and diseases, the effect of *S*-nitrosoglutathione (GSNO) on HXK A structure and activity was studied. To focus on the catalytic domain, yeast HXK A was used because it has a significant homology to the mammalian domain that contains both the regulatory and catalytic sites. Biologically relevant [GSNO]/[HXK] caused a significant decrease in V_{max} with glucose (but not with fructose), along with oxidation of 5 Met and nitration of 4 Tyr. Preincubation of HXK with glucose abrogated the effect of GSNO whereas fructose was ineffective. These results are interpreted by considering the tight binding of glucose to the enzyme as opposed to that of fructose. The segment comprised from amino acids 304 to 306 contained the most modifications. Given that this sequence is highly conserved in HXK from various species, a decline in activity is expected when a high-affinity substrate is presented.

Considering that changes in primary structure are envisioned at high [GSNO]/[HXK] ratios, like those present under normal conditions, it could be hypothesized that the high concentration of hexokinase present in fast growing tumors may serve not only to sustain high glycolysis rates, but also to minimize protein damage that might result in activity decline, compromising energy metabolism.

Keywords: Nitrosoglutathione – Hexokinase – Structure – Activity – Oxygen radicals – Nitrogen radicals – Proteomics – Tumor – Glycolysis

Introduction

Hexokinase (EC 2.7.1.1) is an important glycolytic enzyme that catalyzes the first step of the glycolytic pathway, i.e., the phosphorylation of keto- and aldohexoses (e.g. glucose, mannose and fructose) using MgATP as the phosphoryl donor (Griffin et al., 1991; Middleton, 1990). In rapidly growing tumor cells, the enzyme hexokinase is markedly elevated and 50–80% of the total activity is bound to the outer mitochondrial membrane (Bustamante et al., 1981; Parry and Pedersen, 1983), where it has preferred access to mitochondrially generated ATP (Arora and Pedersen, 1988). In vertebrates there are four major isoenzymes, commonly referred to as types I–IV (Katzen and Schimke, 1965). Structurally, mammalian hexokinases consist of a very small *N*-terminal hydrophobic membrane-binding domain (amino acids 1–12) followed by two highly similar domains of 450 residues, each with a mass of 50 kDa, which share close to a 68% amino acid sequence homology. Based on the amino acid sequence, there is a significant identity between the mammalian forms and yeast hexokinases (Andreone et al., 1989; Arora et al., 1990; Griffin et al., 1991) supporting the gene duplication-gene fusion hypothesis for the evolution of the 100-kDa from the 50-kDa yeast enzymes (Colowick, 1973; Ureta, 1982). It was believed that in mammals, the first domain had lost its catalytic activity and had evolved into a regulatory domain (amino acids 13–475) involved in product inhibition by glucose-6-phosphate (Schwab and Wilson, 1989; White and Wilson, 1987). The *C*-terminal half of the brain enzyme had been shown to account for all its catalytic activity (White and Wilson, 1989). More recently this view has been challenged by demonstrating that the *C*-terminal half is specialized not only for catalysis but also for product inhibition (Arora et al., 1993), probably involved at controlling the fraction of soluble and bound enzyme (Arora et al., 1993). These observations indicated that mammalian hexokinase probably evolved from a 50-kDa hexokinase marine species that had already acquired the capacity for catalysis and product regulation (Mochizuki and Hori, 1976, 1977).

In yeast there are three different hexokinase isoenzymes: hexokinase PI (gene HXK1), PII (gene HXKB),

and glucokinase (gene GLK1). All three proteins have a molecular mass of about 50-kDa. The isoenzymes named A and B (hexokinase PI and PII, respectively) share a 76% overall homology of the amino acid sequence, and these isoenzymes are known to exist as dimers (Frolich et al., 1985; Kopetzki et al., 1985). Yeast hexokinases share a 35% amino acid homology compared to the *C*-terminus end of the mammalian ones, and the glucose- and ATP-binding domains for the tumor, brain, and liver hexokinases had been deduced from amino acid comparisons (Andreone et al., 1989; Griffin et al., 1991) with that of the yeast enzyme, for which the X-ray structure is known (Anderson et al., 1978; Bennett and Steitz, 1980).

Although it is known that changes in the activity and/or binding of mammalian hexokinases have been attributed to play a role in several human diseases (Barrie et al., 1979; Magnani et al., 1985; Valentine et al., 1967; Vionnet et al., 1992), limited studies had been undertaken to evaluate the effect of mitochondrial reactive oxygen and nitrogen species on this enzyme considering that mitochondria are a source of oxygen- and nitrogen-centered radicals (Giulivi et al., 1999; Giulivi, 2003) and that hexokinase is bound to the outer mitochondrial membrane (Wilson, 2003). Given that an overproduction and/or lack of adequate antioxidant support may lead to damage of several critical biomolecules, we investigated the role of a relatively abundant *S*-nitrosothiol (*S*-nitrosoglutathione or GSNO) on hexokinase structure and activity. Our lab has found that mitochondria contain about 200 μM *S*-nitrosoglutathione (Steffen et al., 2001). The homolytic and heterolytic cleavage of this molecule may result in the formation of nitric oxide as well as other reactive radicals, which may modify the primary structure of hexokinase. To this end, we investigated the modifications introduced in the primary structure of yeast hexokinase (as a sole model for the catalytic and product inhibition domain of mammalian hexokinases) by GSNO, and the impact of these modifications on its activity.

Materials and methods

Materials

S-nitrosoglutathione was prepared according to the method described by Hart (1985) and stored at −80 °C, as described before (Steffen et al., 2001). Stock solutions (10 mg/ml) were prepared before running the experiments and kept in the dark on ice.

Yeast hexokinase (9.86 mg/ml) was purchased from Worthington Biochemical Corporation (Lakewood, NJ). This suspension is supplied as a mixture of isoenzymes A and B. The mixture of isoenzymes was separated by using the procedure described by Womack et al. (1973), which is based on the differential adsorption of hexokinase isoenzymes to hydroxyapatite. Hexokinase A fraction was eluted with 0.1 M potassium phosphate buffer, pH 6.8. The specific activity was determined using glucose and fructose as substrates to ascertain purity. The ratio of activities obtained for the substrates glucose/fructose was 2.7 ± 0.3.

Cresol red was obtained from Lancaster Synthesis, Inc. (Pelham, NH), magnesium chloride from Mallinckrodt Chemical, Inc. (Paris, KY), and glycylglycine from Mann Research Laboratories, Inc. (New York, NY). D-glucose, D-fructose, and ATP were obtained from Sigma (St. Louis, MO). Concentrated hydrochloric acid, sodium hydroxide, and the components of the PBS buffer (sodium chloride, potassium chloride, sodium phosphate dibasic, and potassium phosphate monobasic) were all purchased from Fisher (Fair Lawn, NJ). Double-distilled, deionized water was used as the solvent in all cases (unless otherwise specified) and was acquired from a Barnstead Nanopure water filtration system.

Preparation of stock assay solution

The assay method used was based on that described by Giulivi et al. (1999). Seven microlitres of a 0.006% cresol red and 1.6% $MgCl_2 \cdot 6H_2O$ solution were combined with 1.5 ml of 0.1 M ATP (both solutions prepared fresh daily). The resulting solution was then neutralized with 0.1 M NaOH until a magenta-purple color was achieved. To this, 3 ml of 0.1 M glycylglycine buffer (adjusted to pH 9.0 with NaOH) was added, and the volume was brought to 60 ml with doubly deionized water. This stock assay solution was prepared fresh daily and kept on ice throughout each day.

Hexokinase incubation

To this end, 0.5 μM hexokinase A in PBS (pH 7.5) was treated with different amounts of GSNO (as indicated in Fig. 2) or with equal volume of double-distilled water used as vehicle for the GSNO-treated samples. The solutions were incubated in the dark (wrapped in aluminum foil) at 25 °C for one hour. After incubation, each solution was placed on ice for evaluation of enzymatic activities.

Assay procedure

In a 1 ml-cuvette, 1.25 ml of the stock assay solution was combined with 200 μl of glucose or fructose solutions of varying concentrations (see below *Determination of* K_m *and* V_{max}), at a fixed ATP · Mg concentration of 3 mM. The resulting solution was incubated in a Cary 1E UV-Visible Spectrophotometer until the absorbance at 572 nm remained constant. At time zero, an aliquot of hexokinase control or GSNO-treated hexokinase was added, and the absorbance was measured at 572 nm using the Cary WinUV Kinetics Application. The temperature of the reaction mixtures was measured using a Novex PowerEase 500 and recorded for later use. The initial velocity of each reaction (in optical density units/min) was determined by calculating the slope of each curve obtained using the Cary kinetics program.

Adjustment for temperature and determination of activity

Because the cresol red indicator is very sensitive to temperature changes, the temperature must remain constant during each assay, and the crude reaction rate must be multiplied by a temperature factor if the reaction is not run at 30 °C. Darrow and Colowick (1962) provided the formula for this factor: $2.2^{(30-t)/10}$, where t is the temperature at which the reaction takes place. By multiplying the crude initial velocity by this factor, differences in temperature between trials were accounted for in our procedure. A standard curve was used to convert the temperature-adjusted initial velocity (in optical density units/min) to initial velocity in International Units, or μmoles of acid formed/min. The Cary WinUV Concentration Application was used to measure the absorbance at 572 nm of five different samples, each containing 1.25 ml stock assay solution, 200 μl glucose or fructose, and 50 μl of HCl with concentrations ranging from 12.5 to

75 mM. Fifty microlitres doubly deionized water was added to create a blank with which to zero the spectrophotometer before measurement of the other five samples. A plot of μmoles of acid vs. absorbance (in OD) was constructed, and the slope of the regression line passing through the origin was obtained. The temperature-adjusted initial velocities for each trial were then converted to initial velocities in IU by dividing each temperature-adjusted value by the slope of the standard curve. A new standard curve was constructed each day to ensure precise conversion.

Determination of K_m and V_{max}

Initial velocities (in IU) were determined for both hexokinase control and GSNO-treated hexokinase reactions run with varying limiting concentrations of glucose and fructose. Seven different glucose solutions ranging from 0.0015 to 0.2 M and seven fructose solutions ranging from 0.012 to 0.768 M were used in this process. For each hexose concentration, three trials were run with the hexokinase control and three with GSNO-treated hexokinase. The mean initial velocities for each concentration of fructose or glucose were calculated, and five Lineweaver-Burk plots fitted with regression lines (from each of the five trials) were constructed for each of the four conditions (i.e. control hexokinase with glucose, control hexokinase with fructose, GSNO-treated hexokinase with glucose, and GSNO-treated hexokinase with fructose). From the resulting Lineweaver-Burk plots, the K_m and V_{max} were determined, their values being equal to $-1/x$-intercept of the regression line and $1/y$-intercept of the regression line, respectively. Each pair of K_m and V_{max} values for hexokinase control and GSNO-treated hexokinase for one type of hexose substrate were obtained from data that was all collected in one day; thus, the K_m and V_{max} values among the four conditions were compared using paired *t*-tests.

Primary structure modifications

Hexokinase was incubated as described before, and aliquots from each condition (control or GSNO-treated) were extensively dialyzed against PBS, concentrated on Centricom tubes (10-kDa MW cut-off), and then separated by 2-Dimensional gel electrophoresis. The procedure essentially followed the one described in Elfering et al. (2002). The first-dimensional IEF was performed on precast 18-cm IPG strips (Amersham Pharmacia Biotech) at 20 °C with a maximum current setting of 50 μA/strip using an Amersham Pharmacia IPGphor IEF unit. Commercial strips with linear immobilized pH 3–10 gradient were used for isoelectric focusing. These strips were wetted with rehydration buffer containing 2 M thiourea, 7 M urea, 4% CHAPS, 0.5% Triton X-100, 100 mM DTT and 0.4% Pharmalytes, pH 3–10, overnight, in a leveled acrylic strip holder. A low voltage of 30 V was applied during rehydration. After rehydration, IEF run was carried out using the manufacturer's conditions for linear strips using a power supply EPS 3500 XL. Before carrying out the second dimensional sodium dodecyl sulfate-polyacrylamide gel electrophoresis (SDS-PAGE), the strips were subjected to a two-step equilibration. The first was with an equilibration buffer consisting of 6 M urea, 30% glycerol, 2% SDS, 50 mM Tris–HCI (pH 6.8), and 1% w/v DTT. The second step was with a buffer consisting of 6 M urea, 30% glycerol, 2% SDS, 50 mM Tris–HCI (pH 8.8), and 2.5% w/v iodoacetamide. After the IPG strips were transferred onto the second-dimensional SDS-PAGE gel a molecular weight marker strip was included and the strips were sealed in place with 0.75% agarose. SDS-PAGE was performed on 1.0 mm thick 10% polyacrylamide gels at a constant voltage at 13 °C for 5 h using a Hoefer SE600. The gels were stained with silver by following the subsequent protocol: gels were fixed in 50% methanol, 5% acetic acid in water for 30 min followed by washing in 50% methanol in water for 10 min. Then, they were washed again with water for 60 min and sensitized with 0.02% sodium thiosulfate for 2 min. After rinsing the gels twice with water for 1 min each, they were incubated in chilled 0.1% silver nitrate for 40 min at 4 °C. After discarding the silver nitrate and rinsing with two changes of distilled water for 1 min each, the gels were developed in 0.04% formalin (35% formaldehyde in water) in 2% sodium carbonate. When the desired intensity was attained, the developer was discarded and the gel incubated with either 1.46% EDTA disodium dihydrate or 1% acetic acid for 10 min to stop the development. The staining procedure was completed by three rinses with water for 5 min each. Stained gels were scanned using a Kodak Imager (Sunnyvale, CA, USA).

Silver-stained stained protein spots were excised manually with a sterile scalpel blade and transferred to a sterile microcentrifuge tube. Each excised spot was destained, washed, reduced with DTT, alkylated with iodocetamide, and digested in-gel with trypsin. The peptide extraction was performed with ammonium bicarbonate and acetonitrile. Samples were speed vacuumed to dryness after proteolytic digestion and then reconstituted to 15 μl with 95:5, water:acetonitrile, 0.1% trifluoroacetic acid (TFA), vortexed gently and centrifuged at $2000 \times g$ for 30 seconds. Desalting/concentration procedure was performed by using C18 ZipTip®, according to Millipore (Billerica, MA) instructions. A C18 resin was hydrated with 2×10 μl aliquots of 50:50, H_2O:acetonitrile, 0.1% TFA and then equilibrated with 2×10 μl aliquots of aqueous 0.1% TFA. Peptides were bound to C18 by pipetting up and down in the sample 5 times with the pipettor set to 10 μl. Desalting was performed by pipetting 5×10 μl aliquots of aqueous 0.1% TFA through the resin. Elution was performed by pipetting 1.5 μl of 60:40, H_2O:acetonitrile, 0.1% TFA over the resin 3–4 times. One microlitre of the extracted sample from each tube was dispensed onto a MALDI sample plate along with 1 μl of matrix solution consisting of 10-mg/ml α-cyano-4-hydroxycinnamic acid (Sigma-Aldrich, St. Louis, MO) in 0.1% TFA, and 50% acetonitrile and spotted on a MALDI target. Mass analyses were obtained using a PerSeptive Biosystems Voyager-DE STR MALDI-TOF-MS (Framingham, MA, USA) located at the Mass Spectrometry Facility (University of Minnesota). The samples were allowed to dry under ambient conditions. For each sample, the average of 256 spectra was acquired in the delayed extraction and reflector mode. The average of four scans (each containing 64 spectra) that passed the accepted criterion of peak intensity was automatically selected and saved. Spectra were automatically calibrated upon acquisition using a two-point calibration with residual porcine trypsin autolytic fragments (842.51 and 2210.10 [M + W] ions). Assignment of peaks was done manually; measured peptide masses were excluded if their masses corresponded to trypsin autodigestion products or if they were from identified proteins adjacent to the spot being analyzed. The fragments were analyzed against the SWISSPROT and NCBI nonredundant databases using MS-Fit (Protein Prospector; UCSF, San Francisco, CA, USA) and peptide mapping (Profound; version 4.10.5; Rockefeller University). All mass searches were performed using a mass window between 1000 and 100,000 Da, and included human, rat and mouse sequences. The search parameters allowed for oxidation of methionine, *N*-terminal acetylation, carboxyamidomethylation of cysteine, and phosphorylation of serine, threonine and tyrosine.

Results and discussion

1. Characterization of purified hexokinase A from commercially available yeast hexokinase suspension

Commercially available hexokinase is a mixture of yeast hexokinases A and B. For example, ''yeast hexokinase'' from Boehringer seem to be constituted mainly by hexokinase A by all biochemical criteria utilized by Womack et al. (1973). The suspension provided by Sigma is constituted by almost equal parts of each isoform (Prof. Rajiv Bhat, personal communication), whereas that of Worthington is in average 0.5–1.0 of hexokinase B to A

(protein ratios), in agreement with others (Lazarus et al., 1966). Considering that the contribution of each isoform changes from batch to batch, we purified hexokinase A from the mixture provided by Worthington. Hexokinase A was isolated from the suspension by using the procedure described by Womack et al. (1973). By following this method, we obtained two fractions with specific activities (average of 3 preparations) of 280 U/mg protein (hexokinase A) and 750 U/mg protein (hexokinase B).

A tryptic digest obtained from the hexokinase A fraction was used to evaluate its homogeneity by mass spectrometry. Yeast hexokinase A (P04806) ranked at the top of the protein list with a MOWSE score of 2.3×10^8. The matched peptides covered a significant portion of the protein (50%, calculated as 243 detected/485 amino acids; Fig. 1). Given the high sensitivity of mass spectrometry (fmol), other minor proteins were detected with significant lower MOWSE score values. They were the 26S proteasome regulatory subunit 6A (P33297; MOWSE 4059), the 26S proteasome regulatory subunit RPN9 (Q04062; MOWSE 3434), hexokinase B (P04807; MOWSE 2591), cytosolic NADP-dependent isocitrate dehydrogenase (P41939; MOWSE 2078), and hypothetical protein in PEX 12 (Q0437; MOWSE 1121).

In a parallel approach, Eadie-Scatchard plots of hexokinase activity would provide an indication of isoform con-

Index Number: **134355**

Acc. #: P04806 **Species:** YEAST **Name:** Hexokinase A (Hexokinase PI)

p*I* of Protein: **5.3**

Protein MW: **53739**

Amino Acid Composition: **A32 C4 D36 E35 F17 G42 H9 I33 K39 L48 M13 N18 P25 Q15 R18 S24 T29 V28 W4 Y16**

```
1          11         21         31         41         51         61         71
MVHLGPKKPQ ARKGSMADVP KELMDEIHQL EDMFTVDSET LRKVVKHFID ELNKGLTKKG GNIPMIPGWV MEFPTGKESG
81         91         101        111        121        131        141        151
NYLAIDLGGT NLRVVLVKLS GNHTFDTTQS KYKLPHDMRT TKHQEELWSF IADSLKDFMV EQELLNTKDT LPLGFTFSYP
161        171        181        191        201        211        221        231
ASQNKINEGI LQRWTKGFDI PNVEGHDVVP LLQNEISKRE LPIEIVALIN DTVGTLIASY YTDPETKMGV IFGTGVNGAF
241        251        261        271        281        291        301        311
YDVVSDIEKL EGKLADDIPS NSPMAINCEY GSFDNEHLVL PRTKYDVAVD EQSPRPGQQA FEKMTSGYYL GELLRLVLLE
321        331        341        351        361        371        381        391
LNEKGLMLKD QDLSKLKQPY IMDTSYPARI EDDPFENLED TDDIFQKDFG VKTTLPERKL IRRLCELIGT RAARLAVCGI
401        411        421        431        441        451        461        471
AAICQKRGYK TGHIAADGSV YNKYPGFKEA AAKGLRDIYG WTGDASKDPI TIVPAEDGSG AGAAVIAALS EKRIAEGKSL
481
GIIGA
```

Fig. 1. Primary sequence coverage of hexokinase A. The masses of the tryptic digest of hexokinase A were processed by using ProteinProspector software. Contaminating masses were those obtained with the same solutions as the control but without protein, and subjected to the same treatment (trypsin digestion). Database sequence shown in black; matched amino acids shown in bold

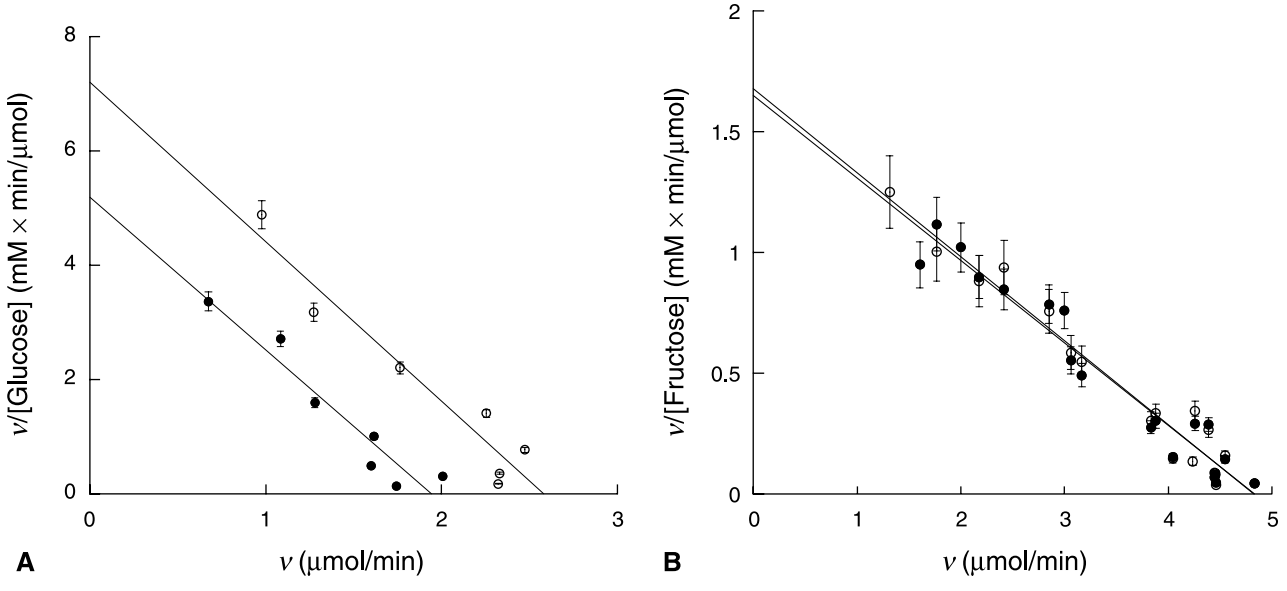

Fig. 2. Eadie-Scatchard plots of hexokinase A activity with glucose and fructose as substrates. The activity of control (open circles) and GSNO-treated (closed circles) hexokinase A was tested with glucose (**A**) or fructose (**B**) as substrate. For experimental details see Materials and methods

Table 1. Comparison of experimental kinetic constants of yeast hexokinase A with published values

Parameter	Hexokinase A	Hexokinase B	This study
V_{max}, μmol × (min × mg protein)$^{-1}$	275[a] 225[c]	900[a] 730[b] 850[c]	280 ± 5
K_m (glucose), mM	0.3[a]	0.6[a] 0.31[b]	0.47 ± 0.06
V_{max} (fructose)/ V_{max} (glucose)	2.0–2.3[d] 2.0[a] 3.0[a] 2.8–3.0[e]	1.3[a] 1.1[a] 1.4[b] 1.0–1.2[e]	2.7 ± 0.3

[a] Ramel et al. (1971)
[b] Ma et al. (1989a)
[c] Womack et al. (1973)
[d] Rustum (1971)
[e] Lazarus et al. (1966)

tribution in terms of activity, if the data did not conform to a single Michaelis-Menten equation. When the observed rates were plotted according to the Eadie-Scatchard equation over a wide range of glucose concentrations, all plots were linear (Fig. 2; open circles), indicating that the quantitative contribution of hexokinase A was predominant. The kinetic constants (observed K_m and observed V_{max}) calculated from the plots were similar to those published for purified hexokinases A and B (Table 1).

Our results indicated that the major isoenzyme in our purified fraction was constituted by hexokinase A based on the mass spectrometry data and the values of the experimental kinetic constants.

2. *Effect of GSNO incubation on hexokinase A activity*

To evaluate the effect of GSNO on hexokinase A activity, several molar ratios were tested. Given that rat liver mitochondria contain about 200 μM GSNO and the hexokinase content can be estimated at less than 1 μM[1], a physiologically relevant ratio of [GSNO]/[hexokinase] would be 40 and higher. Considering that the glycolytic capacity of several tumors correlates with mitochondrial hexokinase activity (Bustamante et al., 1981), relevant ratios of [GSNO]/[hexokinase] for fast growth rate tumors[2] (equal to or faster than one month) would be lower than 200.

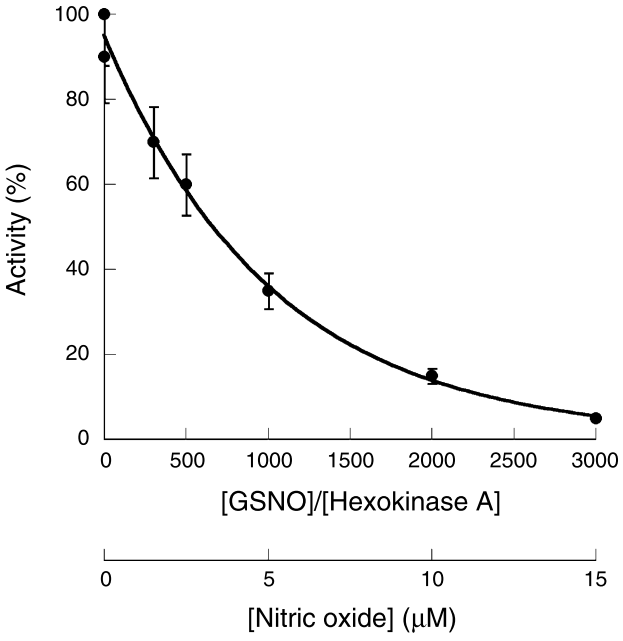

Fig. 3. Effect of GSNO on hexokinase A activity. Purified hexokinase A was treated with various concentrations of GSNO. The activity of each sample was tested as described in detail under the same Section. The range of hexokinase content for control tissues ranges from 1 (liver; Bustamante et al., 1981; Gots and Bessman, 1974) to 80 (brain; Johnson, 1960) nmol glucose/min mg protein. For tumors with high glycolytic rate, the range was considered from 20 to 400 nmol glucose/min mg protein (Bustamante et al., 1981)

Those tumors with slow growth rate would have intermediate values, overlapping at each end with fast growth tumors and normal tissues (Fig. 3). In principle, we chose molar ratios of [GSNO]/[hexokinase A] spanning these biologically relevant conditions (Fig. 3).

Exposure of hexokinase to GSNO for 1 h at 25 °C in the dark, at the indicated molar ratios (Fig. 3), presented a concentration-dependent decline of the V_{max} (Fig. 3). Under these conditions, no protein fragmentation and/or aggregation was observed as judged by the lack of higher molecular weight aggregates (polymers) or smear (fragmentation) in SDS-PAGE (under reducing and nonreducing conditions) stained with silver.

About 50% activity decrease was observed at [GSNO]/[hexokinase] ratio of 670, resulting in a GSNO concentration of 335 μM. Although this concentration might seem high compared to that of hexokinase, it is appropriate to indicate that the decay of GSNO under our experimental conditions was about 1%/h (evaluated by spectrophotometry at 330 nm; experimental first order rate constant of $2.8 \times 10^{-6}\ s^{-1}$), indicating that at the end of the incubation period, only 3.35 μM GSNO had been decomposed to nitric oxide and other metabolites.

[1] Hexokinase is present at low activity in liver, where glucokinase is the predominat glucose phosphorylationg actvity.
[2] Growth rate expressed in terms of months that either elapse between transplantations or that are needed for a solid tumor to reach 1.5 cm diameter according to Bustamante et al. (1981).

Table 2. Kinetic parameters of hexokinase A with glucose or fructose as substrates after GSNO incubation

Hexokinase	Glucose		Fructose	
	K_m (mM)	V_m (μmol/min mg protein)	K_m (mM)	V_m (μmol/min mg protein)
Control	0.47 ± 0.06	280 ± 5	2.9 ± 0.2	756 ± 13
GSNO-treated	0.3 ± 0.1	$169 \pm 2^*$	2.9 ± 0.3	749 ± 11

[a] Each of the above K_m values represents the mean ± standard error of five independent trials. K_m values for each trial were determined by measuring the initial velocities of reactions catalyzed by either control hexokinase or GSNO-treated hexokinase and run with varying limiting concentrations of either glucose or fructose substrate. Lineweaver-Burk plots were constructed, and K_m values were calculated by taking the negative reciprocal of the x-intercept of the linear regression line of each plot. The V_{max} values were calculated by taking the reciprocal of the y-intercept of the linear regression line of each plot. The significance level was set at 0.05. $^*p < 0.01$

Given that hexokinase utilizes aldohexoses as well as ketohexoses as substrates, we performed experiments to evaluate the kinetic parameters that might have been affected by GSNO exposure (Fig. 3, closed circles and Table 2). These experiments were performed at a molar ratio of GSNO-to-hexokinase of 500:1 to evaluate the effect of GSNO under normal conditions. The only parameter statistically significant different obtained after GSNO exposure was the V_{max} with glucose. No difference was found with the apparent K_m for ATP or glucose, or with the apparent K_m and V_{max} with fructose. These results are best explained by the weaker binding of fructose than glucose at the same active center. The modifications introduced by GSNO might affect the tight binding of glucose to the enzyme, but not that of fructose.

Supporting this view, the preincubation of hexokinase A with 10 mM glucose ($20 \times K_m$) abrogated the partial inactivation caused by GSNO whereas 60 mM fructose ($20 \times K_m$) was ineffective at preventing the GSNO-mediated decrease of V_{max} with glucose[3]. This differential effect of glucose vs. fructose in terms of protecting the active site has also been described for an alkylating agent, *N*-bromoacetylgalactosamine; in contrast, this alkylating agent promoted the same activity loss with either substrate (Otieno et al., 1975).

[3] These concentrations of glucose and fructose are lower than those used in similar experiments Otieno et al. (1975) (10^{-2} M). The reason to use saturating concentrations as opposed to higher ones, was to minimize potential artifactual reactions between the sugar and GSNO-derived metabolites.

It is worth noting that the exposure of hexokinase A to GSNO might have resulted in either a subpopulation of enzyme with no noticeable activity or a mixture of

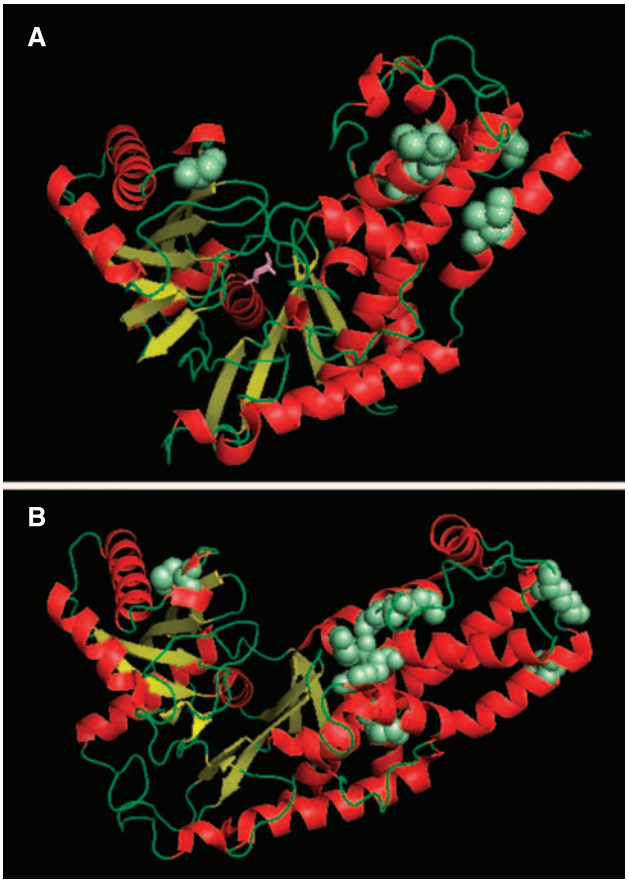

Fig. 4. Three-dimensional structure of hexokinase. Hexokinase A chain is colored according the structure (alpha-helix, red; beta sheet, yellow; random coil, green). The model is in a closed (1BDG.pbd with glucose in pink sticks; **A**) or open (1IG8.pdb; **B**) conformation. The active site resides between the two domains. The amino acids that were modified by GSNO treatment are shown in the space-filled structure. The structures were originally obtained with RasMol v.2.7.2.1.1, refined by using PyMol v. 0.98

Table 3. Differential amino acid modifications in hexokinase A after GSNO treatment evaluated by mass spectrometry

Tryptic segment (amino acid number)	Modification
22–42	Met 24 oxidized
111–122	Met 118 oxidized
304–315	Met 304 oxidized, Tyr 308 nitrated, Tyr 309 nitrated
304–315	Met 304 oxidized
325–337	Met 327 oxidized
336–349	Met 342 oxidized
338–349	Met342, Tyr 340 or Tyr 346 nitrated
338–349	Met 342 oxidized, Tyr 340 nitrated, Tyr 346 nitrated

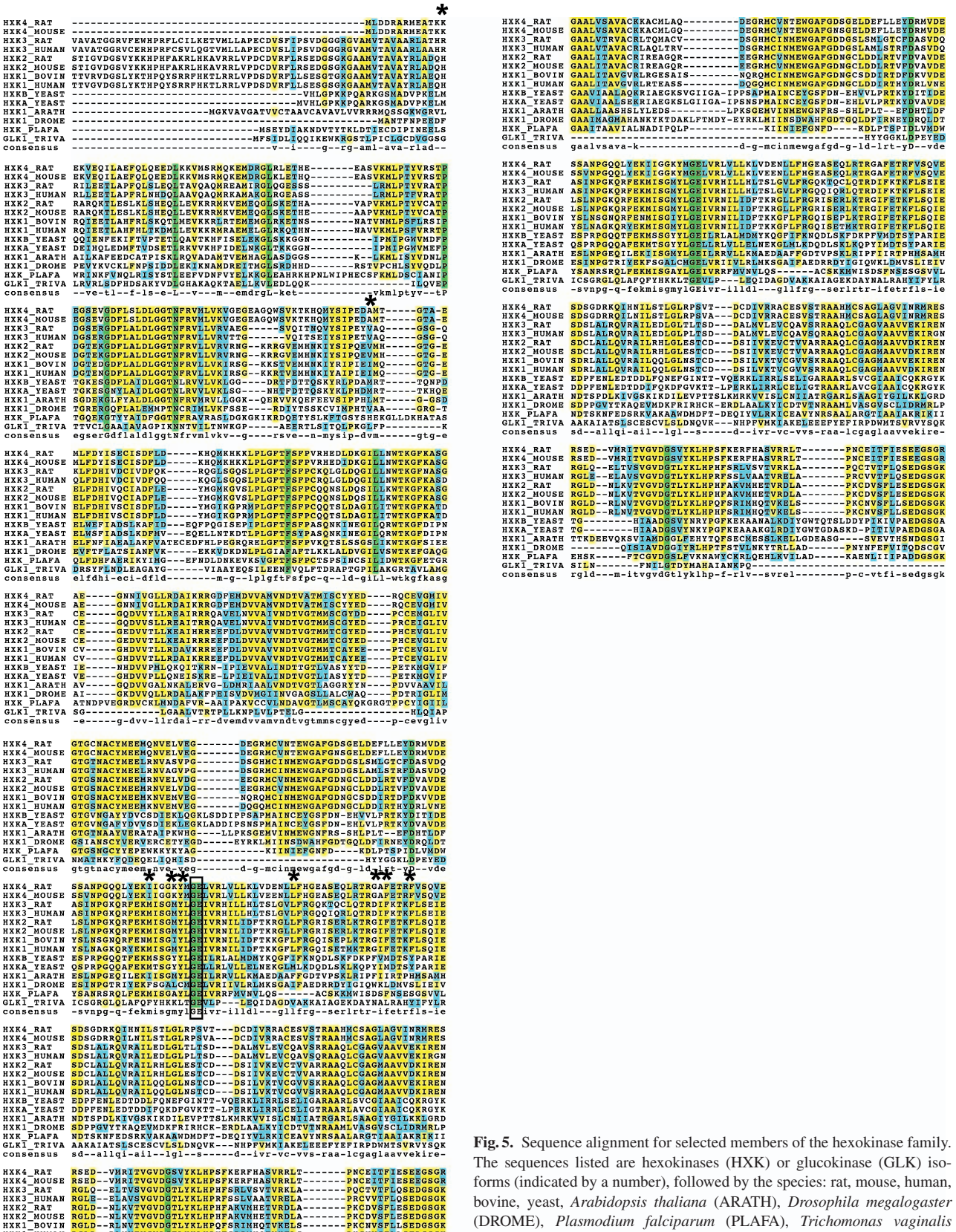

Fig. 5. Sequence alignment for selected members of the hexokinase family. The sequences listed are hexokinases (HXK) or glucokinase (GLK) isoforms (indicated by a number), followed by the species: rat, mouse, human, bovine, yeast, *Arabidopsis thaliana* (ARATH), *Drosophila megalogaster* (DROME), *Plasmodium falciparum* (PLAFA), *Trichomonas vaginalis* (TRIVA). Green shaded residues are 100% match when all sequences were aligned by using ClustalW. Blue and yellow shaded residues are highly conserved and similar, respectively. An asterisk indicates residues modified by GSNO treatment

enzymes with lower specific activity. Our results are compatible with the first alternative because our data (Fig. 2, closed circles) were fitted to one single line ($r^2 = 0.99$) indicating that there is a homogeneous population of enzyme that essentially kept the original specific activity.

3. Effect of substrate binding on GSNO incubation

It is known that hexokinase, crystallized as a complex with glucose, has a conformation that is dramatically different from that crystallized in the absence of glucose. Comparison of the high-resolution structures shows that one lobe of the molecule is rotated by 12 degrees relative to the other lobe, resulting in movements of as much as 8 Å in the polypeptide backbone and closing the cleft between the lobes into which glucose is bound (Bennett and Steitz, 1978). The conformational change is produced by the binding of glucose (McDonald et al., 1979) and is essential for catalysis (Anderson et al., 1978) and thus provides an example of induced fit (Fig. 4). The surface area of the hexokinase A-glucose complex exposed to solvent is smaller than that of native hexokinase. To evaluate if there was any change in the inactivation of the enzyme in the presence of GSNO in its open (without substrates) or closed (with substrates) conformations, hexokinase was preincubated with either ATP or glucose at saturating concentrations, and then exposed to GSNO treatment. Both substrates ATP and glucose prevented the inactivation of the enzyme by GSNO treatment, indicating that the decrease in the surface area when the enzyme is in its close conformation plays a key role at shielding labile residues from GSNO attack. However, preincubation with fructose did not result in a significant protection. Similar results were obtained with hexokinase in the presence of various alkylating agents and they were attributed to the weaker binding of fructose to hexokinase when compared to that of glucose (Otieno et al., 1975).

4. GSNO-mediated changes in hexokinase A primary structure

To evaluate the modifications of hexokinase A after GSNO incubation, hexokinase samples were dialyzed extensively to remove any by-products, trypsinized in solution, and subjected to MALDI-ToF analyses. The masses of the tryptic digests that were not present in control samples were analyzed for modifications, namely, nitration of tyrosine and oxidation of methioneine residues (Table 3).

The treatment of hexokinase with GSNO at a molar ratio of 500 (GSNO-to-hexokinase) resulted in the oxidation of 5 Met and nitration of 4 Tyr (Table 3). When these residues were identified in the primary and secondary structures (Figs. 1 and 4), it was evident that most of the affected residues were present in beta-turns and loops.

The glucose-binding domain for hexokinase has been deduced from X-ray studies and it includes the following residues Ser-158, Asp-211, Asn-237, Glu-269, and Glu-302 (Bennett and Steitz, 1980; Kuser et al., 2000). Initial glucose recognition followed by closure of the cleft between the two HK domains brings amino acid residues of the small domain, i.e., Thr172 and Lys173, within hydrogen-bonding interaction distances of the substrate (Kuser et al., 2000). The ATP binding pattern was defined by five sequence motifs: phosphate 1 (residues 82–103), connect 1 (203–223), phosphate 2 (229–248), adenosine (411–439), and connect 2 (453–473) with a number of Gly, Ser, Thr, and Asp residues being strictly conserved amongst all compared sequences (Kuser et al., 2000). None of the modified residues found by MS was among the residues involved in the binding of either ATP or glucose (compare above residue numbers with those in Table 3). However, there are two amino acids which might have been affected indirectly by the GSNO-mediated modifications: one, Glu-302 (involved in the binding of O-1 atom of glucose; Kuser et al., 2000) is close to Met-304, an amino acid found oxidized after GSNO incubation (Table 3). Two, a high number of Gly are conserved in hexokinases (Gly76, 80, 88, 89, 154, 233, 235, 297, 307, 311, 418, 461; Kuser et al., 2000). These residues are located at the ends of β-strands of α-helices, changing the direction of the chain (Kuser et al., 2000). Their conservation probably gives the hexokinase molecule the flexibility necessary for binding glucose and ATP (Kuser et al., 2000). In this regard, Gly-307 and 311 are relatively close to Tyr-308 and Tyr-309, both residues found nitrated in GSNO-treated hexokinase. The introduction of two nitro groups with the consequent pK_a change of the phenoxyl group might have hindered the apparent flexibility that this Gly has in its original milieu. Of note, these amino acids found as targets of GSNO-derived species, responsible for the maintenance of a critical structure to sustain an adequate function, were all present at the large domain of hexokinase, only a few amino acids apart (304 through 309). Met-304 is highly conserved among several species as well as Tyr-309 suggesting their importance in hexokinase function (Fig. 5). In addition, substitution of amino acids in this segment resulted in a protein with negligible activity; for example, mutating Ser-305 for Pro in yeast strains

Table 4. Cys-containing tryptic peptides in control and GSNO-treated hexokinase A

m/z (monoisotopic)	Amino acid		Database sequence
	Start	End	
960.50	384	391	LCELIGTR
1417.69	383	394	RLCELIGTRAAR
1500.72	380	391	LIRRLCELIGTR

decreased the activity by 50-fold (Ma et al., 1989b) or substituting Glu-742 (equivalent to Glu-302 in yeast) for Gly or Ala in tumor hexokinase increased the K_m for glucose by 14-fold with only a 6% of the V_{max} (Arora et al., 1991).

Oxidative and nitrative modifications to amino acids other than Tyr and Met could had been expected. In this regard, Cys residues are particularly susceptible to nitrative/oxidative damage, with the potential of yielding sulfinic acid (SOH), sulfenic acid (SO_2H), disulfides, *S*-nitroso moieties (SNO), among others. From the four Cys present in hexokinase A (268, 385, 398, and 404) only one was detected by mass spectrometry of the tryptic digests, i.e., Cys-385 (Table 4). Three overlapping peptides were obtained in both control and GSNO-treated samples indicating that – at least – this Cys had not undergone any modification.

Given that the proteomic approach involves the reduction of Cys with DTT followed by alkylation with iodoacetamide, it was not possible to evaluate the presence of disulfide bonds. Running 10% non-reducing SDS-PAGE allowed us to test for intermolecular disulfide bond formation. No evidence was obtained for the formation of dimers or polymers of multiples of 50 kDa.

Although *S*-nitrosation of Cys might have caused the inactivation of hexokinase, two experiments excluded this possibility: one, addition of dithiotreitol, to promote the heterolytic cleavage of the putative Cy*S*–NO bond, or irradiation at 330 nm for 30 min, where the *S*–NO bond absorbs, did not recover significantly the activity.

5. Conclusions

The control points at the glycolytic pathway are catalyzed by hexokinase, phosphofructokinase-1 and pyruvate kinase. As the entry point of the glycolysis, hexokinase plays a crucial role. Thus, cellular situations that may lead to its inactivation may result in cellular damage. We have demonstrated that hexokinase is particularly susceptible to protein structure modifications when exposed to even low concentrations of GSNO. The changes allowed a decrease in activity, which may result in a lower entry flux into the glycolytic pathway, compromising cellular energy balance. This is especially important in energy metabolism of tumors in which the rate of glycolysis is high (Warburg et al., 1924). Assuming that in tumors, the concentration of GSNO is similar to that of normal tissues, then hexokinase inactivation is more likely to occur under the latter condition because there is more GSNO available per hexokinase molecule. It is interesting to propose that tumor cells may increase the concentration of hexokinase not only to sustain a high rate of glycolysis but also to minimize putative nitrative damage to the protein. Highly glycolytic tumors, by increasing hexokinase concentration (Bustamante et al., 1981) (and its binding to the outer mitochondrial membrane; Johnson, 1960; Rose and Warms, 1967) assure a steady supply of phosphorylated glucose (as an entry point for glycolysis) despite changes in oxidative/nitrative stress.

Hexokinase modifications under in vivo conditions might result in the same amino acid modifications as in our in vitro experiments, for the binding of the protein to the outer mitochondrial membrane has not been considered (which may result in protection or actually more damage if nitrative stress is propagated through membrane lipids). Future experiments will address the issues of binding and activity of hexokinase during nitrative stress.

Acknowledgements

The Research Corporation Award (CC5675), NIH ES012691, NIH ES005707 and the Elsa Pardee Foundation supported this study. We thank the technical assistance of Mrs. Virginia Haynes, Ms. Sarah Poe, Ms. Sarah Elfering, Ms. Anya Gybina, and Mr. Nicholas Hoxmeier.

References

Anderson CM, Stenkamp RE, McDonald RC, Steitz TA (1978) A refined model of the sugar binding site of yeast hexokinase B. J Mol Biol 123: 207–219

Andreone TL, Printz RL, Pilkis SJ, Magnuson MA, Granner DK (1989) The amino acid sequence of rat liver glucokinase deduced from cloned cDNA. J Biol Chem 264: 363–369

Arora KK, Pedersen PL (1988) Functional significance of mitochondrial bound hexokinase in tumor cell metabolism. Evidence for preferential phosphorylation of glucose by intramitochondrially generated ATP. J Biol Chem 263: 17422–17428

Arora KK, Fanciulli M, Pedersen PL (1990) Glucose phosphorylation in tumor cells. Cloning, sequencing, and overexpression in active form of a full-length cDNA encoding a mitochondrial bindable form of hexokinase. J Biol Chem 265: 6481–6488

Arora KK, Filburn CR, Pedersen PL (1991) Glucose phosphorylation. Site-directed mutations which impair the catalytic function of hexokinase. J Biol Chem 266: 5359–5362

Arora KK, Filburn CR, Pedersen PL (1993) Structure/function relationships in hexokinase. Site-directed mutational analyses and characterization of overexpressed fragments implicate different functions for the N- and C-terminal halves of the enzyme. J Biol Chem 268: 18259–18266

Barrie SE, Saad EA, Ubatuba S, Da Silva Lacaz P, Harris P (1979) Myocardial enzyme activities in congestive cardiomyopathy. Res Commun Chem Pathol Pharmacol 23: 375–381

Bennett WS Jr, Steitz TA (1978) Glucose-induced conformational change in yeast hexokinase. Proc Natl Acad Sci USA 75: 4848–4852

Bennett WS Jr, Steitz TA (1980) Structure of a complex between yeast hexokinase A and glucose. II. Detailed comparisons of conformation and active site configuration with the native hexokinase B monomer and dimer. J Mol Biol 140: 211–230

Bustamante E, Morris HP, Pedersen PL (1981) Energy metabolism of tumor cells. Requirement for a form of hexokinase with a propensity for mitochondrial binding. J Biol Chem 256: 8699–8704

Colowick SP (1973) Hexokinases. In: Boyer PD (ed) Enzymes, 3rd ed, Vol 9. Academic Press, New York, pp 1–48

Darrow RA, Colowick SP (1962) Hexokinase from baker's yeast. Methods Enzymol 5: 226–235

Elfering SL, Sarkela TM, Giulivi C (2002) Biochemistry of mitochondrial nitric-oxide synthase. J Biol Chem 277: 38079–38086

Frohlich K, Entian K, Mecke D (1985) The primary structure of the yeast hexokinase PII gene (HXK2) which is responsible for glucose repression. Gene (Amst) 36: 105–111

Giulivi C, Boveris A, Cadenas E (1999) Oxygen radicals in mitochondria: critical evaluation of the methodology available for estimating steady-state concentrations of oxygen radicals. In: Gilbert DL, Colton CA (eds) Reactive oxygen species in biological systems: selected topics. Plenum Press, New York, pp 77–102

Giulivi C (2003) Characterization and function of mitochondrial nitric-oxide synthase. Free Radical Biol Med 34: 397–408

Gots RE, Bessman SP (1974) The functional compartmentation of mitochondrial hexokinase. Arch Biochem Biophys 163: 7–14

Griffin LD, Gelb BD, Wheeler DA, Davison D, Adams V, McCabe ER (1991) Mammalian hexokinase 1: evolutionary conservation and structure to function analysis. Genomics 11: 1014–1024

Gupta BL, Nehal M, Baquer NZ (1997) Effect of experimental diabetes on the activities of hexokinase, glucose-6-phosphate dehydrogenase and catecholamines in rat erythrocytes of different ages. Indian J Exp Biol 35: 792–795

Hart T (1985) Some observations concerning the *S*-nitroso and *S*-phenylsulfonyl derivatives of L-cysteine and glutathione. Tetrahedron Lett 26: 2013–2016

Johnson MK (1960) The intracellular distribution of glycolytic and other enzymes in rat-brain homogenates and mitochondrial preparations. Biochem J 77: 610–618

Katzen HM, Schimke RT (1965) Multiple forms of hexokinase in the rat: tissue distribution, age dependency, and properties. Proc Natl Acad Sci USA 54: 1218–1225

Kopetzki E, Entian K, Mecke D (1985) Complete nucleotide sequence of the hexokinase PI gene (HXK1) of *Saccharomyces cerevisiae*. Gene (Amst) 39: 95–102

Kuser PR, Krauchenco S, Antunes OAC, Polikarpov I (2000) The high resolution crystal structure of yeast hexokinase PII with the correct primary sequence provides new insights into its mechanism of action. J Biol Chem 275: 20814–20821

Lazarus NR, Ramel Ah, Rustum YM, Barnard EA (1966) Yeast hexokinase. I. Preparation of the pure enzyme. Biochemistry 5: 4003–4016

Ma H, Bloom LM, Dakin SE, Walsh CT, Botstein D (1989a) The 15 *N*-terminal amino acids of hexokinase II are not required for in vivo function: analysis of a truncated form of hexokinase II in *Saccharomyces cerevisiae*. Proteins 5: 218–223

Ma H, Bloom LM, Zhu Z, Walsh CT, Botstein D (1989b) Isolation and characterization of mutations in the HXK2 gene of *Saccharomyces cerevisiae*. Mol Cell Biol 9: 5630–5642

Magnani M, Stocchi V, Cucchiarini L, Novelli G, Lodi S, Isa L, Fornaini G (1985) Hereditary nonspherocytic hemolytic anemia due to a new hexokinase variant with reduced stability. Blood 66: 690–697

McDonald RC, Steitz TA, Engelman DM (1979) Yeast hexokinase in solution exhibits a large conformational change upon binding glucose or glucose 6-phosphate. Biochemistry 18: 338–342

Middleton RJ (1990) Hexokinases and glucokinases. Biochem Soc Trans 18: 180–183

Mochizuki Y, Hori SH (1976) Hexose 6-phosphate dehydrogenase in starfishes. Comp Biochem Physiol B 54: 489–494

Mochizuki Y, Hori SH (1977) Purification and properties of hexokinase from the starfish, *Asterias amurensis*. J Biochem (Tokyo) 81: 1849–1855

Otieno S, Bhargava AK, Barnard EA, Ramel AH (1975) Yeast hexokinases. VIII. Essential thiols of yeast hexokinase. Alkylation by a substrate-like reagent. Biochemistry 14: 2403–2410

Parry DM, Pedersen PL (1983) Intracellular localization and properties of particulate hexokinase in the Novikoff ascites tumor. Evidence for an outer mitochondrial membrane location. J Biol Chem 258: 10904–10912

Ramel AH, Rustum YM, Jones JG, Barnard EA (1971) Yeast hexokinase. IV. Multiple forms of hexokinase in the yeast cell. Biochemistry 10: 3499–3508

Rose IA, Warms JV (1967) Mitochondrial hexokinase. Release, rebinding, and location. J Biol Chem 242: 1635–1645

Rustum YM, Ramel AH, Barnard EA (1971) The preparation of yeast hexokinases. Prep Biochem 1: 309–329

Schwab DA, Wilson JE (1989) Complete amino acid sequence of rat brain hexokinase, deduced from the cloned cDNA, and proposed structure of a mammalian hexokinase. Proc Natl Acad Sci USA 86: 2563–2567

Steffen M, Sarkela TM, Gybina AA, Steele TW, Traaseth NJ, Kuehl D, Giulivi C (2001) Metabolism of *S*-nitrosoglutathione in intact mitochondria. Biochem J 356: 395–402

Ureta T (1982) The comparative isozymology of vertebrate hexokinases. Comp Biochem Physiol 71B: 549–555

Valentine WN, Oski FA, Paglia DE, Baughan MA, Schneider AS, Naiman JL (1967) Hereditary hemolytic anemia with hexokinase deficiency. Role of hexokinase in erythrocyte aging. N Engl J Med 276: 1–11

Vionnet N, Stoffel M, Takeda J, Yasuda K, Bell GI, Zouali H, Lesage S, Velho G, Iris F, Passa P, Froguel P, Cohen D (1992) Nonsense mutation in the glucokinase gene causes early-onset non-insulin-dependent diabetes mellitus. Nature 356: 721–722

Warburg O, Posener K, Negelein F (1924) Metabolism of carcinoma cells. Biochem Z 152: 309–344

White TK, Wilson JE (1987) Rat brain hexokinase: location of the allosteric regulatory site in a structural domain at the *N*-terminus of the enzyme. Arch Biochem Biophys 269: 402–411

White TK, Wilson JE (1989) Isolation and characterization of the discrete *N*- and *C*-terminal halves of rat brain hexokinase: retention of full catalytic activity in the isolated *C*-terminal half. Arch Biochem Biophys 274: 375–393

Wilson JE (2003) Isozymes of mammalian hexokinase: structure, subcellular localization and metabolic function. J Exp Biol 206: 2049–2057

Womack FC, Welch MK, Nielsen J, Colowick SP (1973) Purification and serological comparison of the yeast hexokinases P-I and P-II. Arch Biochem Biophys 158: 451–457

Authors' address: Dr. Cecilia Giulivi, Department of Molecular Biosciences, University of California, 1311 Haring Hall, One Shields Ave, Davis, CA 95616, U.S.A.,
E-mail: cgiulivi@ucdavis.edu